

Solvent-Free Chemoselective Hydrogenation of Squalene to Squalane

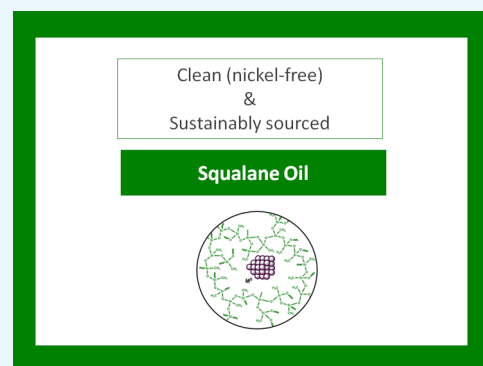
Valerica Pandarus,^{†,‡} Rosaria Ciriminna,[§] François Béland,^{*,†} Mario Pagliaro,^{*,§,§} and Serge Kaliaguine^{*,‡}

[†]SiliCycle, 2500, Parc-Technologique Boulevard, Quebec City, Quebec, Canada G1P 4S6

[‡]Department of Chemical Engineering, Laval University, 2325 Rue de l'Université, Quebec City, Quebec, Canada G1V 0A6

[§]Istituto per lo Studio dei Materiali Nanostrutturati, CNR, via U. La Malfa 153, 90146 Palermo, Italy

ABSTRACT: Squalene is selectively and entirely converted into squalane over the spherical sol–gel-entrapped Pd catalyst *SiliaCat* Pd(0) under solvent-free and mild reaction conditions of 3 bar H₂ and 70 °C. The catalyst was reused successfully in eight consecutive cycles, with palladium leaching values <2 ppm, opening the route to sustainable and less-expensive hydrogenation of phytosqualene with important sustainability consequences.



INTRODUCTION

Obtained by full hydrogenation of the highly unsaturated all-(*E*) linear terpenoid squalene ((6*E*,10*E*,14*E*,18*E*)-2,6,10,15,19,23-hexamethyltetracos-2,6,10,14,18,22-hexaene), an immune system stimulant and anticarcinogenic and antioxidant agent widely used in traditional medicine and nutraceutical products,¹ squalane (C₃₀H₆₂) is a clear and nonirritant oil widely and increasingly employed by the cosmetic, pharmaceutical, and nutraceutical industries.² For example, thanks to its exceptional capacity to penetrate and impart flexibility to the human skin, as well as to vehiculate and increase the absorption of other active substances,³ squalane is used to formulate top cosmetic products including creams, hair conditioners, lotions, lipsticks, sunscreens, bath oils, and foundations. Today, this valued substance is mainly derived from vegetable sources including olive oil (46% of the overall market share in 2015)⁴ and biotechnology squalene from sugarcane (10%), even though a significant fraction (40%) is still obtained from deep sea shark liver oil (Scheme 1).

Sugarcane squalene is obtained via Pd-catalyzed dimerization of sesquiterpene (*E*)- β -farnesene derived from sucrose fermentation over genetically engineered strains of *Saccharomyces cerevisiae*,⁵ affording a consistent composition of 94% phytosqualene along with 3.5% isosqualane and 2.5% monocyclosqualane.⁶ Table 1 summarizes the advantages and disadvantages of heterogeneously catalyzed hydrogenation processes carried out in industry over the commonly used supported metal catalysts.

Accounting for about 40% of the overall production cost,⁷ the squalene hydrogenation process is carried out over nickel-kieselguhr catalyst under the solvent-free reaction conditions of 4 bar H₂ at 200 °C⁸ or over more costly Pd/C of 70 bar H₂ at

160 °C. In the former case, extensive leaching of Ni requires prolonged purification of the hydrogenated product over silica and other adsorbent materials to meet the maximum acceptable levels of highly toxic nickel compounds (Ni²⁺ and Ni⁰) in a cosmetic product (0.2 ppm). In the latter, the surface-derivatized nature of conventional commercial Pd/C catalyst leads to a rapid decrease in the catalytic performance.⁹ Furthermore, if squalene originating from olive oil is used,¹⁰ the inevitable presence of residual waxes requires first a “winterization” step to precipitate wax, followed by hydrogenation in two steps: first under 5 bar of H₂ pressure for 3–4 h, followed by another 3 h at 30 bar H₂ to afford complete saturation.

We recently reported that the heterogeneous hydrogenation of squalene dissolved in ethanol over *SiliaCat* Pd(0) selectively affords high yields of squalane using an ultralow amount of palladium loading (0.02 mmol/g of squalene) under remarkably mild conditions (1 bar H₂, 30 °C, or 50 °C when shorter reaction times are needed).¹⁵ Comprising organosilica catalyst doped with Pd(0) nanocrystals, the catalyst is reusable, with hydrogenation of a lesser pure olive oil squalene (82 wt %) requiring somewhat harsher reaction conditions.

Shortly afterwards, Soni and Sharma in India reported the excellent performance of a Pd/clay catalyst under solvent-free conditions at 200 °C under 4 bar H₂.¹⁶ Complete conversion of squalene to squalane was achieved after 6 h with a Pd loading of approximately 0.06 mmol/g of squalene. Under the said optimized reaction conditions, the catalyst was remarkably

Received: May 18, 2017

Accepted: July 13, 2017

Published: July 26, 2017

Scheme 1. Squalene Purity and Composition Issues, Depending on Its Origin

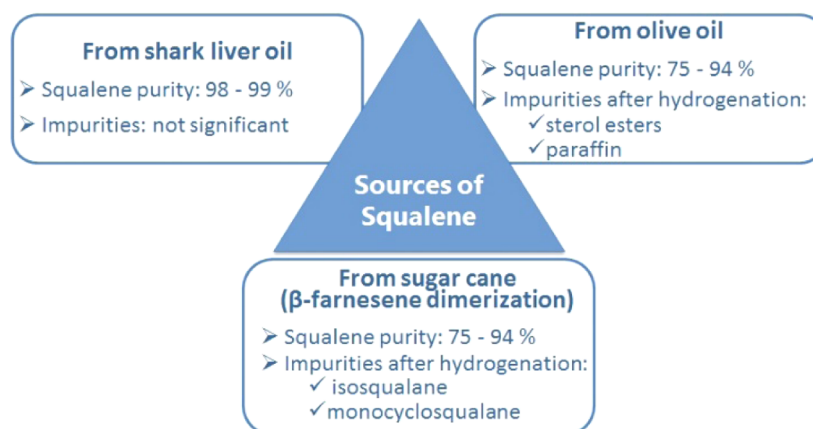
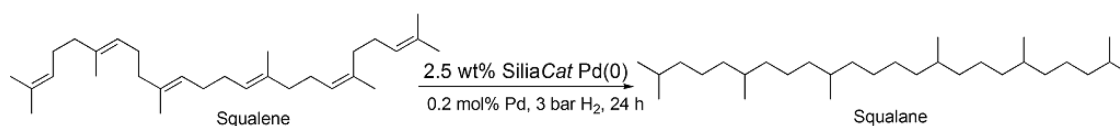


Table 1. Advantages and Disadvantages of Industrial Squalene Hydrogenation over Commonly Used Supported Metal Catalyst

heterogeneous catalysts	industrial hydrogenation of squalene	advantage/disadvantage
Pt catalyst ^{11,12}	shark-liver squalene: in diethyl ether under H ₂ pressure solvent-free, 1 bar H ₂ , 190 °C	high amount of expensive Pt catalyst toxic solvent
Ni-Raney ¹³	shark-liver squalene: solvent-free, 10 bar H ₂ , 170 °C, 3 h	low-cost Ni catalyst harsher conditions in presence or in absence of solvent
Ni-kieselguhr ⁸	shark-liver squalene: solvent-free, 4 bar H ₂ , 200 °C, 3–4 h	high level of the Ni leached into the squalane product
Pricat Ni 61/15P (Ni/alumina-kieselguhr) ¹⁴	vegetable squalene: in 2-PrOH, 24 bar H ₂ , 150 °C, 16 h	extensive purification is required to remove most of the Ni leached
Pd/C ¹⁴	vegetable squalene: in heptane, 58 bar H ₂ , 80 °C, 16 h in 2-PrOH, 150 bar H ₂ , 160 °C	harsher conditions

Scheme 2. Solvent-Free Hydrogenation of Squalene over SiliaCat Pd(0) under Optimized Reaction Conditions



stable and an ultralow amount of Pd leached into the product (0.0311 ppm), which established the best squalene hydrogenation catalyst ever reported. Now, we show how the full hydrogenation of all-*E* linear squalene into valued squalane is achieved over the spherical sol–gel-entrapped Pd catalyst SiliaCat Pd(0) under solvent-free and mild reaction conditions (3 bar H₂ and 70 °C) over a 0.2 mol % Pd loading in the form of 2.5 wt % SiliaCat Pd(0) catalyst (Scheme 2) using two squalenes of a different origin and purity.

The catalyst is extensively reusable, with palladium leaching values <2 ppm, opening the route to an easier and low-cost hydrogenation of squalene.

RESULTS AND DISCUSSION

SiliaCat Pd(0) is a heterogeneous catalyst obtained via the alcohol-free sol–gel polycondensation of alkoxy silanes such as methyltrimethoxysilane (MTES).¹⁷ The hydrophobic character of the organosilica support protects the Pd nanoparticles (NPs) against oxidation, increases the stability against moisture, and increases the catalytic activity of the catalyst under mild conditions.^{18,19}

Following advances anticipated in 2011 for which the spherical morphology of the silica microparticles could be beneficial to catalysis,²⁰ the catalyst is now available in spherical morphology (Figure 1, left).

The newly prepared catalyst comprises catalytically active Pd⁰ NPs encapsulated within a spherical mesoporous organically

modified silica matrix. The presence of highly dispersed average 3.1 nm palladium NPs was clearly revealed by the TEM analysis (Figure 1, right). The crystalline nature of the active nanophase is evident from the X-ray diffraction (XRD) pattern of the catalyst powder (Figure 2, right) characteristic of the face-centered cubic (fcc) structure of metallic Pd for which a typical 2.6 nm crystal domain was calculated using the Debye–Scherrer equation²¹ from the line broadening of majority (111) reflections (Table 2).

Table 2. Load and Pd NP Size of the Spherical SiliaCat Pd(0)

catalyst	palladium loading (wt %)	TEM (NP size)	XRD (NP size)
MeSiO _{1.5}			
SiliaCat Pd(0) (Pd ⁰ /MeSiO _{1.5})	2.5	3.1 nm	2.6 nm

The amorphous nature of the spherical 100% MeSiO_{1.5} undoped material used as entrapping NPs matrix was confirmed by the characteristic wide XRD diffractogram of the blank spherical MeSiO_{1.5} xerogel devoid of metal NPs (Figure 2, left).

The Brunauer–Emmett–Teller (BET) and Barrett–Joyner–Halenda (BJH) values of specific surface area, pore size, and pore volume of undoped organosilica microspheres and SiliaCat Pd(0) catalyst are given in Table 3.

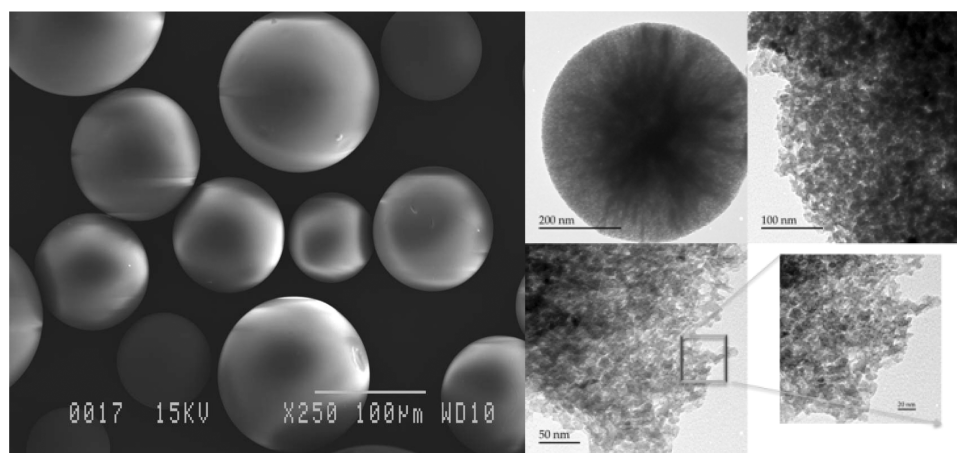


Figure 1. Scanning electron microscopy (left) and transmission electron microscopy (TEM) (right) images of SiliaCat Pd(0) spherical palladium catalyst used throughout this study.

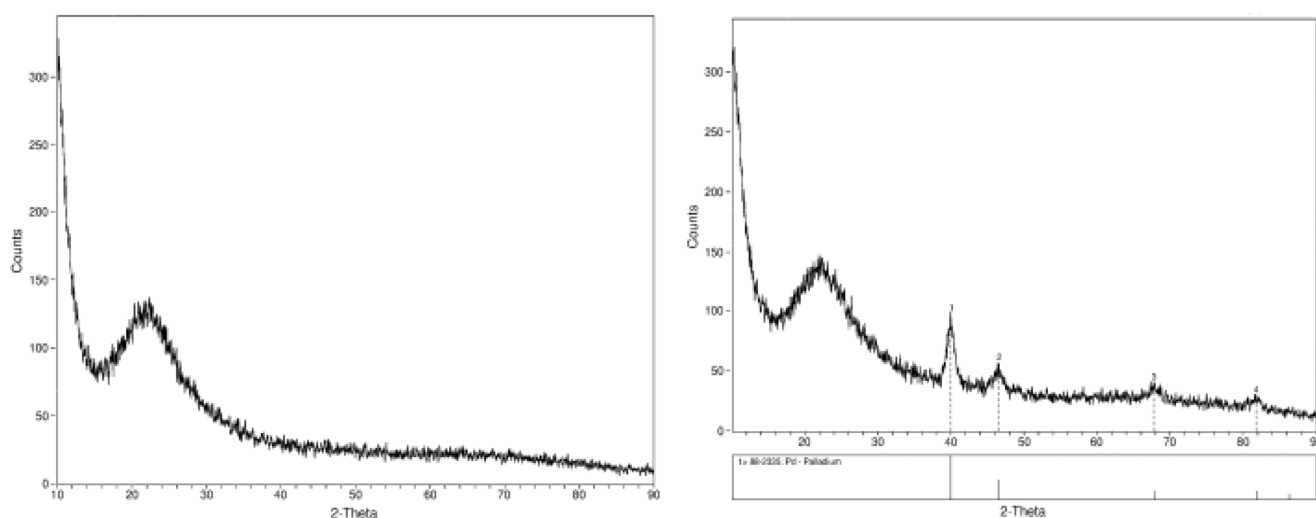


Figure 2. Powder XRD patterns of MeSiO_{1.5} blank material (left) and the Pd/MeSiO_{1.5} NP organosilica catalyst SiliaCat Pd(0) (right).

Table 3. Textural Properties of Spherical SiliaCat Pd(0) and Blank Support

catalyst	Pd loading (wt %)	N ₂ adsorption isotherms		
		BET surface (m ² /g)	pore volume (cm ³ /g)	pore size (nm)
MeSiO _{1.5}		835	1.27	6.1
SiliaCat Pd(0)	2.5	402	0.8	8.0
Pd ⁰ /MeSiO _{1.5}				

The type IV N₂ adsorption–desorption isotherms of both materials are typical of mesoporous materials.²² The organosilica blank (Figure 3, left) presents a large BET surface area (>800 m²/g) and 6.0 nm average pore diameter with a narrow size distribution of mesopores capable of adsorbing a large volume of cryogenic nitrogen (>1.2 cm³/g). On the other hand, the Pd/MeSiO_{1.5} catalyst (Figure 3, right) has a lower BET surface area (average 400 m²/g) and a broader pore size distribution centered at 8.0 nm.

The ²⁹Si magic angle spinning (MAS) NMR spectra of the support and the catalyst in Figure 4 were analyzed according to the chemical shifts of organotrialkoxysilanes for which the Si atoms appear as Tⁿ bands type, where *n* is the number of siloxane bonds of the Si atom.²³ The absence of any signal at

−40 ppm related to ethoxy groups derived from nonhydrolyzed MTES and the presence of signals only at −56 ppm (T², MeSi(OSi)₂OH) and −66 ppm (T³, MeSi(OSi)₃) correspond to almost complete hydrolysis of the MTES organosiloxane precursor.²⁴

Effect of Reaction Temperature. Table 4 shows the outcomes of the solvent-free hydrogenation of squalene under the conditions of Scheme 2 using squalene of a different origin and purity (98 wt % from Sigma-Aldrich and 82 wt % from an olive squalene manufacturer).

First, entries 2–8 in Table 4 show that in each case the experimental values of leached Pd (and Si) in the crude product were <2 ppm (threshold value for palladium in oils for cosmetic and food products in the United States).

Entries 1 and 2 show that the hydrogenation of high-purity squalene with complete conversion and 99% squalane selectivity was smoothly achieved at 70 °C after 24 h reaction. However, entry 3 shows that when squalene obtained from olive oil in 82 wt % purity was used in place of pure squalene, the substrate conversion into squalane was only 39%. Furthermore, entries 3–8 show evidence that the hydrogenation of olive oil-derived squalene requires harsher conditions than that of pure squalene, with temperature having a crucial effect. Rise in the temperature from 70 to 180 °C increases the selectivity in squalane from 39

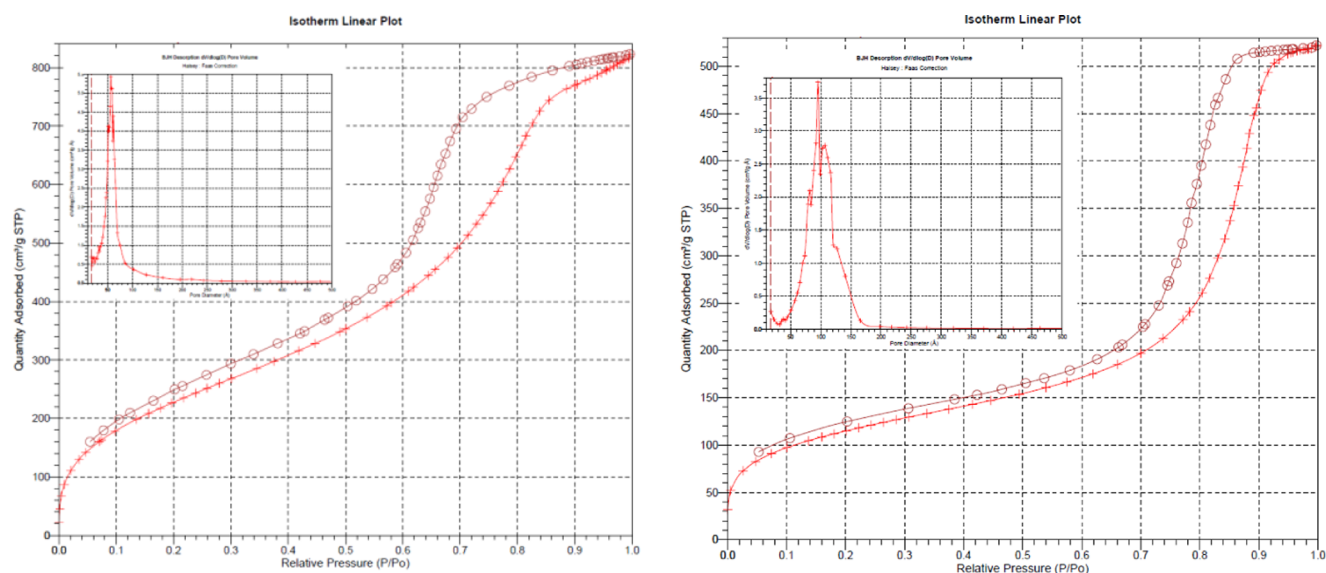


Figure 3. N₂ adsorption and desorption isotherms and BJH desorption pore size distribution of MeSiO_{1.5} blank support (left) and spherical SiliaCat Pd(0) (right).

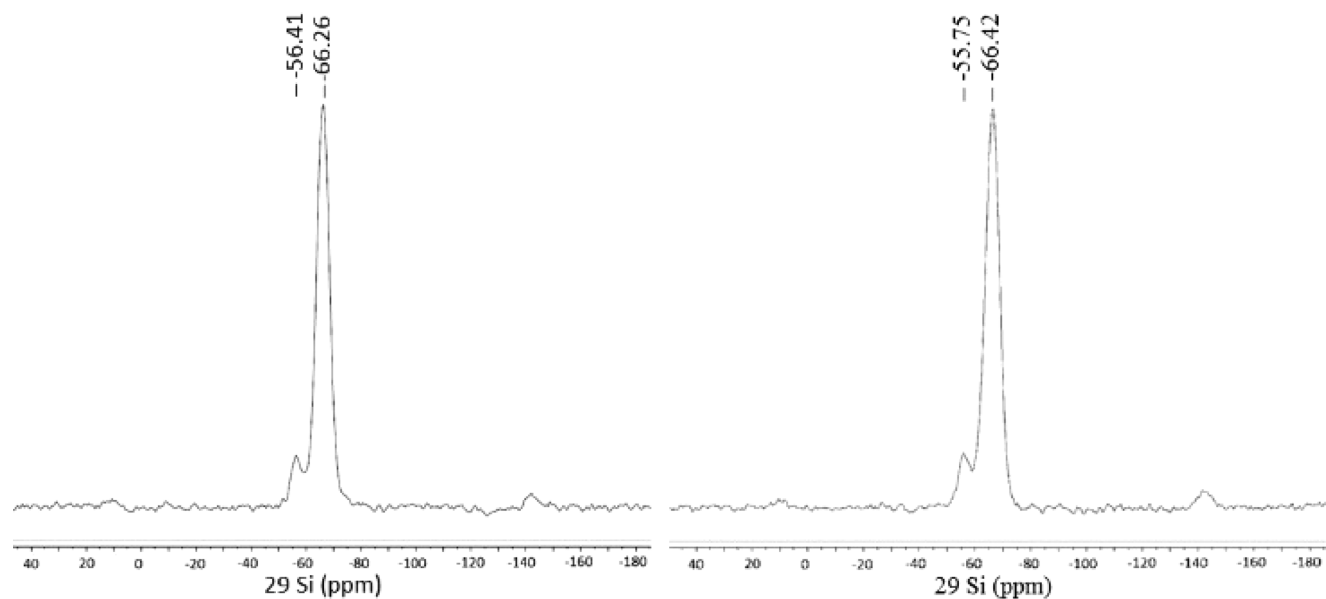


Figure 4. ²⁹Si MAS NMR spectra of MeSiO_{1.5} blank support (left) and spherical SiliaCat Pd(0) (right).

to 100%. At 150 °C and under 3 bar H₂, the conversion of olive oil squalene to squalane with 98% selectivity was achieved after 24 h (entry 7). At 180 °C, however, complete conversion was obtained after only 16 h (entry 8).

Squalene conversion and selectivity to squalane were calculated and plotted against the reaction temperature (Figure 5) revealing the dependence of squalane selectivity on the latter parameter.

Effect of H₂ Pressure. To study the effect of hydrogen pressure on the solvent-free catalytic hydrogenation of olive squalene (82% pure) over 0.2 mol % Pd, the H₂ pressure was increased from 3 to 20 bar and the conversion of squalene to squalane at 180 °C was evaluated at different reaction times (Table 5).

From the data in Table 5, the values for squalane conversion and selectivity after 4, 7, and 16 h were calculated and plotted

against the H₂ pressure (Figure 6), revealing the dependence of squalane selectivity on the H₂ pressure.

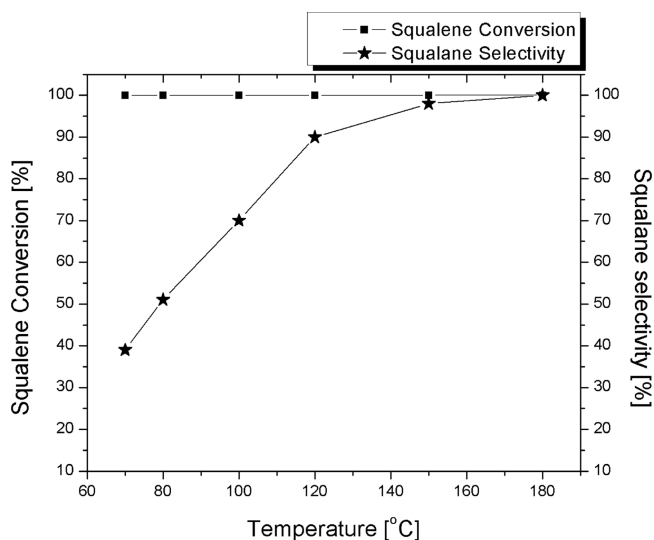
Figure 6 shows that after 4 h, raising the H₂ pressure from 3 to 20 bar improves the squalane selectivity from 30 to 98%. Similarly, after 7 h reaction time, bringing the hydrogen pressure to 20 bar enhances the squalane selectivity from slightly more than 50% to complete selectivity with the full conversion of squalene over a very low Pd loading (0.005 mmol Pd/g of substrate).

After 16 h and at 180 °C, complete conversion of olive oil squalene to squalane was obtained at all of the H₂ pressures applied (3, 6, and 10 bar). The effect of the hydrogen pressure suggests that, as expected from a truly heterogeneous reaction involving a solid (the catalyst) and a gaseous reactant (H₂), the rate of reaction is strongly dependent on the solubility of the hydrogen in the reaction mixture over the range of pressure studied. The hydrogen pressure impacts directly on the H₂

Table 4. Conversion, Selectivity, and Metal Leaching Values in the Solvent-Free Hydrogenation of Squalene of Different Purities over SiliaCat Pd(0)^a

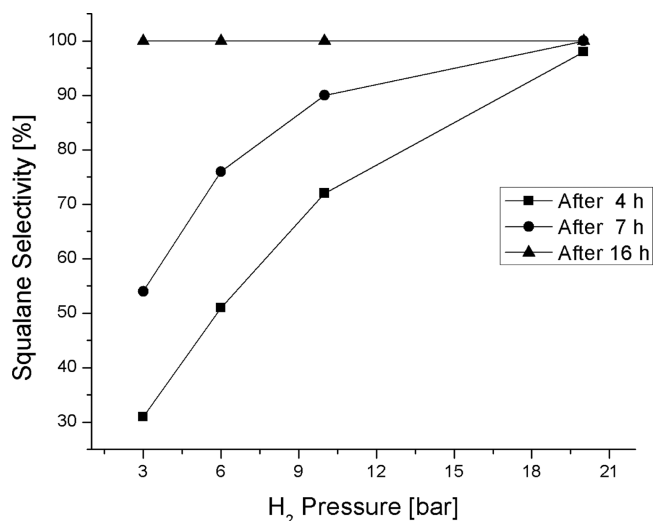
entry	squalene (purity, %)	T (°C)	conversion/selectivity ^b (%)	leaching ^c (mg/kg)	
				Pd	Si
1	98	50	100/45		
2	98	70	100/99	1.57	1.98
3	82	70	100/39	1.00	2.01
4	82	80	100/51	0.99	0.59
5	82	100	100/70	0.39	0.59
6	82	120	100/90	0.1	0.30
7	82	150	100/98	1.27	0.39
8 ^d	82	180	100/100	0.81	1.01

^aReaction conditions: 3 bar H₂ at different temperatures over 0.2 mol % SiliaCat Pd(0) for 24 h. ^bSqualene conversion/squalene selectivity evaluated by gas chromatography–mass spectrometry (GC–MS) analysis. ^cLeaching of Pd and Si was assessed by inductively coupled plasma–optical emission spectroscopy (ICP–OES) analysis in 1,1,2-trichloroethane.²⁶ ^dSixteen hours reaction time.

**Figure 5.** Effect of temperature in hydrogenation of olive squalene (82 wt % purity).**Table 5.** Conversion and Selectivity of Squalene in the Solvent-Free Hydrogenation of Olive Squalene over SiliaCat Pd(0) under Different Hydrogen Pressure^a

entry	H ₂ pressure (bar)	T (h)	conversion/selectivity ^b (%)
1	3	4	100/31
2	3	7	100/54
3	3	16	100/100
4	6	4	100/42
5	6	7	100/76
6	6	16	100/100
7	10	4	100/72
8	10	7	100/90
9	10	16	100/100
10	20	4	100/98
11	20	7	100/100

^aReaction conditions: 180 °C, H₂ pressure as in table entries, 0.2 mol % SiliaCat Pd(0). ^bSqualene conversion/squalene selectivity evaluated by GC–MS analysis.

**Figure 6.** Effect of hydrogen pressure on hydrogenation of 82% pure olive oil squalene.

diffusion through the gas and liquid films at the bubble–liquid interface and therefore the diffusion through the bulk liquid phase and the liquid film at the liquid–solid interface, as well as the reaction rate on the catalytic solid surface. A high reaction pressure also affects the kinetics of squalene adsorption and squalene desorption from the Pd⁰ NPs (the GC–MS analysis clearly showed a fast primary hydrogenation of squalene even after 4 h, revealing the presence of intermediate partially hydrogenated products of squalene).

Effect of Catalyst Loading. Table 6 shows the results obtained by varying the reaction palladium loading using once again 82 wt % olive oil-derived squalene under different reaction conditions. Entry 1 displays that over 0.5 mol % Pd catalyst, corresponding to 0.012 mmol Pd entrapped in SiliaCat Pd(0) per gram of squalene, the substrate conversion to squalane at 120 °C under 3 bar H₂ pressure is quantitative after 20 h. At the same H₂ pressure and increasing the temperature to 150 °C (entry 2) and 180 °C (entry 3), the conversion becomes quantitative after 16 and 7 h, respectively, showing once again the large impact of the reaction temperature on the rate of squalene hydrogenation.

Entries 4–6 in Table 6 show that reactions at 180 °C, with over 0.2 mol % Pd catalyst (corresponding to 0.005 mmol Pd/g of squalene) under 3–10 bar H₂ pressure, result in quantitative conversion of squalene to squalane after 16 h. Under higher H₂ pressure (20 bar), the rate of the squalene hydrogenation reaction increased with 98% squalene selectivity observed after 4 h only, and the quantitative conversion to squalane after 7 h (entries 7 and 8).

Finally, lowering the SiliaCat Pd(0) load to 0.1 mol % Pd only (corresponding to 0.0024 mmol Pd/g of squalene), the quantitative conversion to squalane could be achieved only at a higher temperature and an H₂ pressure (entries 9–12) at 180 °C, whereas over 0.05 mol % Pd (corresponding to 0.0012 mmol Pd/g of squalene), the selectivity to squalane after 24 h was 58% only under 10 bar H₂ (entry 13) and 84% under 20 bar H₂ pressure (entry 14) despite full conversion of squalene. The relevance of the reaction parameters on the solvent-free squalene hydrogenation to squalane over SiliaCat Pd(0), thus, follows the order: Pd concentration > temperature > pressure.

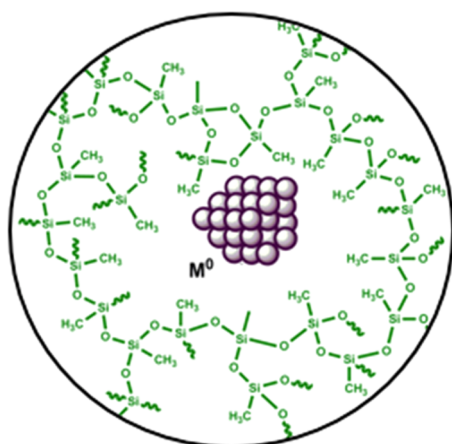
We ascribe the high catalytic activity of the newly developed spherical SiliaCat Pd(0) catalyst to (i) the large mesoporosity,

Table 6. Conversion of Squalene and Squalane Selectivity in the Solvent-Free Hydrogenation of Olive Oil Squalene over Different Amounts of SiliaCat Pd(0)

entry	SilicaCat Pd(0) (wt % catalyst/mol % Pd) ^a	experimental conditions				conversion/selectivity ^b (%)	leaching ^c (mg/kg)	
		T (°C)	H ₂ (bar)	t (h)	Pd		Si	
1	5/0.5	120	3	20	100/100			
2	5/0.5	150	3	16	100/100	0.73	1.55	
3	5/0.5	180	3	7	100/100	0.74	1.17	
4	2/0.2	180	3	16	100/100	0.81	1.01	
5	2/0.2	180	6	16	100/100	0.78	0.91	
6	2/0.2	180	10	16	100/100	0.78	0.86	
7	2/0.2	180	20	4	100/98	0.92	0.67	
8	2/0.2	180	20	7	100/100	0.83	0.66	
9	1/0.1	180	10	16	100/95			
10	1/0.1	180	10	24	100/98	0.69	0.86	
11	1/0.1	180	20	7	100/69	0.82	0.76	
12	1/0.1	180	20	16	100/100	0.72	0.70	
13	0.5/0.05	180	10	24	100/58	0.81	0.65	
14	0.5/0.05	180	20	24	100/84	0.69	0.71	

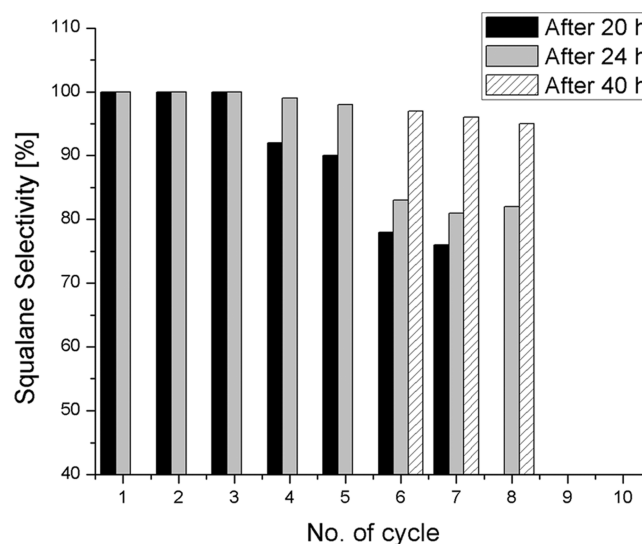
^aCatalyst–squalene mass ratio/palladium–squalene molar ratio. ^bSqualene conversion/squalane selectivity evaluated by GC–MS. ^cLeaching of Pd and Si was assessed by ICP-OES analysis in 1,1,2-trichloroethane.

(ii) hydrophobicity of the organosilica matrix protecting the NPs tightly entrapped within the sol–gel cages (Figure 7), and (iii) the enhanced morphology with its much larger surface-to-volume ratio (*S/V*) when compared with analogous sol–gel catalyst comprising irregular xerogel microparticles.

**Figure 7.** Molecular structure of the SiliaCat Pd(0) catalyst.

The dramatic dependence of the hydrogenation rate on the reaction temperature may be explained by squalene/squalane diffusion limitations through the inner porosity of the solid catalyst and subsequent access to the active sites on the Pd NPs.

Catalyst Stability. The reusability of the catalyst was evaluated in several consecutive multigram hydrogenation reactions of 82% pure olive oil squalene (50 mL, 43.13 g, 105 mmol) using 0.5 mol % SiliaCat Pd(0) under solvent-free conditions at 150 °C under 3 bar hydrogen pressure. In each cycle, once the maximum conversion of squalene to squalane was achieved, the catalyst was collected by filtration, washed with tetrahydrofuran (three times during 10 min) to remove the wax impurities present in the olive oil squalene, dried at room temperature and reused in the subsequent cycle. Figure 8 shows that the spherical SiliaCat Pd(0) heterogeneous catalyst was reused successfully in eight consecutive cycles.

**Figure 8.** Reusability of SiliaCat Pd(0) in squalene hydrogenation.

In the first three consecutive reaction tests, complete conversion was obtained in 20 h, after which the squalane selectivity progressively decreased to reach high values after 24 h (cycles 4 and 5) and after 40 h (cycles 6–8). The longer reaction time was applied to ensure a high squalane conversion.

In brief, the SiliaCat Pd(0) heterogeneous catalyst was stable and robust, which is a crucially important factor for practical applications in place of conventional Pd/C and Ni-kieselguhr commercial catalysts.

The amounts of Pd and Si leached from the SiliaCat Pd(0) during catalysis were assessed by analyzing via ICP-OES the metal content in the isolated crude product after the filtration of the catalyst.^a Values reported in Tables 4 and 6 show that in each case the values of leached Pd and Si found in the crude product are <2 ppm.

Table 7 summarizes the outcomes of squalene hydrogenation reaction using different heterogeneous catalysts under optimized solvent-free conditions or with the substrate dissolved in alcohol or *n*-heptane. Entry 2 in Table 7 shows that SiliaCat

Table 7. Conversion and Squalane Selectivity in the Hydrogenation of Squalene with Different Purities under Optimized Reaction Conditions over Different Catalysts under Solvent-Free Conditions or Carried Out with the Substrate Dissolved in Solvent^a

entry	catalyst (mol % M) ^b	purity (%)	squalene solution/solvent-free	conversion/selectivity ^c (%)	experimental conditions		
					T (°C)	H ₂ (bar)	t (h)
1	2.5 wt % SiliaCat Pd(0) (0.2)	98	EtOH (1.00 M)	100/99	50	3	24
2		82	EtOH (0.70 M)	100/94	70	3	24
3	2.5 wt % SiliaCat Pd(0) (0.2)	98	solvent-free	100/99	70	3	24
4		82	solvent-free	100/98	150	3	24
5		82	solvent-free	100/100	180	3	16
6 ^d	5 wt % Pd/C (0.2)	82	solvent-free	100/51	150	3	16
7 ^d		82	solvent-free	100/69	150	3	24
8 ^e	5 wt % Pd/C ¹⁴ (1.1)	>80	2-PrOH/heptane (0.64 M)	100/89	85	70	16
9 ^e	5 wt % Pd/C ¹⁴ (0.5)	>80	2-PrOH (0.70 M)	100/99	160	150	
10 ^e	10 wt % Pd/C ¹⁴ (0.4)	>90	heptane (0.50 M)	100/97.5	80	20	16
11 ^e	10 wt % Pd/C ¹⁴ (1.1)	>90	heptane (0.70 M)	100/99	85	60	16
12	6 wt % Pd/clay ¹⁶ (0.6)	98	solvent-free	100/100	300	10	10
13	Ni-Raney ¹⁵ (14.5)	98	solvent-free	100/99	170	10	4

^aExperimental and literature data. ^bPalladium/squalene molar ratio. ^cSqualene conversion/squalene selectivity evaluated by GC–MS. ^dPd/C (5 wt %) from Sigma-Aldrich tested in the same conditions as entry 4. ^eSqualene reaction mixture obtained after dimerization of (*E*)- β -farnesene was passed to hydrogenation step without work-up.

Pd(0) affords the highest yield and selectivity under the mildest reaction conditions.

CONCLUSIONS

The newly developed sol–gel-entrapped Pd catalyst SiliaCat Pd(0) in spherical morphology added in small amount of 0.2 mol % smoothly mediates the chemoselective full hydrogenation of squalene into valued squalane under solvent-free, mild reaction conditions (3 bar H₂ at 70 °C). Catalysis is truly heterogeneous, with values of leached palladium <2 ppm. The catalyst is easily recovered and reused for several consecutive reaction runs with practically no loss of catalytic activity, opening the route to a cleaner and less-expensive hydrogenation of squalene. Compared with numerous other commercial catalysts employed in industry, lower temperatures and pressures are generally required due to several synergistic factors that include easier accessibility of the Pd⁰ NPs entrapped in the inner huge porosity of the hydrophobic organosilica spherical microparticles of enhanced surface/volume ratio. Like organosilica irregular xerogel catalysts of the SiliaCat series,²⁵ the spherical SiliaCat Pd(0) catalyst does not swell or stick to the reactor surface and can be easily handled in air, showing no tendency to ignite upon exposure to air, as happens with conventional Pd/C and related catalysts.

Squalane is an extremely important emollient and bioactive substance with multiple health benefits and its production cost is significantly (40%) impacted by the cost of the hydrogenation process.⁷ Now that phytosqualene biotechnologically derived from sugarcane or extracted from olive oil milling residues is replacing squalene of animal origin,² these findings will further contribute to lowering the cost and increasing the availability of high-quality squalane.

MATERIALS AND METHODS

The squalene samples with different purities (98% from Sigma-Aldrich, 82 wt % from an olive squalene manufacturer) and 5% Pd/C (from Sigma-Aldrich) were used as received. Multigram hydrogenation tests of squalene under maximum pressure of 3 bar H₂ at 120 °C were carried out in an Ace Glass 6437 system equipped with a batch glass reactor. The 500 mL glass reactor

was charged with 250 mL olive squalene (82 wt % purity; 214.5 g, 522.25 mmol) and 4.43 g SiliaCat Pd(0) (2 wt %) for 0.2 mol % Pd. Mechanical stirring was then set at 850 rpm and the reaction mixture was degassed five times, replacing three times the vacuum by Ar and twice Ar with H₂. The hydrogenation reactions conducted at H₂ pressure higher than 3 bar were carried out in a Parr 4848 high-pressure reactor controller equipped with a steel container. The 100 mL steel reactor was charged with 50 mL olive squalene (43.13 g, 105 mmol, 82 wt % purity) and 0.89 g SiliaCat Pd(0) (2.5 wt %) for 0.2 mol % Pd loading. The mixture stirred at 700 rpm was purged with H₂ at 20 bar five times, after which the desired pressure was maintained. The reaction temperature was then raised from 22 °C to the desired reaction temperature and maintained for several hours, after which the reaction mixture was allowed to reach 50 °C and the solid catalyst recuperated by filtration. The reaction conversion and squalane selectivity were assessed by GC–MS.

The GC–MS analysis showed that in cases where the conversion of squalene (molecular weight (MW): 410) to squalane (MW: 422) was incomplete, a large number of intermediate partially hydrogenated products (MW: 412, 414, 416, 418, and 420) were present in the reaction mixture. We thus explored the effects of the reaction temperature, hydrogen pressure, and catalyst loading on conversion and selectivity.

The physical properties of SiliaCat Pd(0) catalyst were determined by nitrogen adsorption, transmission XRD, TEM, ²⁹Si MAS NMR spectroscopy, and ICP-OES. Nitrogen adsorption and desorption isotherms at 77 K were measured using a Micromeritics TriStar II 3020 system. The resulting data were analyzed with the TriStar II 3020 version 3.02 software. Both BJH adsorption and desorption branches were used to calculate the pore size distribution. The XRD analysis was performed on a Siemens D-5000 X-ray diffractometer equipped with a monochromatic Cu K α radiation source ($\lambda = 1.5418$). The spectra were recorded in the 2θ range of 0–30° for the undoped support and of 10–90° for SiliaCat Pd(0) catalyst at a scan speed of 1°/min and a step scan of 0.02°. The powder diffraction file of the International Centre for Diffraction Data

was used to identify the diffraction peaks characteristic of crystalline Pd(0) with a fcc lattice.

The TEM photographs were taken with a JEOL-2010 microscope equipped with a LaB6 electron gun source operated at 200 kV. Solid-state ^{29}Si NMR spectra were recorded on a Bruker Avance spectrometer (Milton, ON, Canada) at a Si frequency of 79.5 MHz. Each time the solid sample was spun at 8 kHz in a 4 mm ZrO rotor. A Hahn echo sequence synchronized with the spinning speed was used while applying a TPPM15 composite pulse decoupling during acquisition. A total of 2400 acquisitions were recorded with a recycling delay of 30 s.

The leaching of Pd and Si was assessed by ICP-OES analysis of the squalane crude product in 1,1,2-trichloroethane (concentration 100 mg/mL) using a PerkinElmer Optima 2100 DV system. The values measured are reported as milligram of Pd and as milligram of Si per kilogram of squalane oil.

AUTHOR INFORMATION

Corresponding Authors

*E-mail: FrancoisBeland@silicycle.com (F.B.).

*E-mail: mario.pagliaro@cnr.it (M.P.).

*E-mail: Serge.Kaliaguine@gch.ulaval.ca (S.K.).

ORCID

Mario Pagliaro: 0000-0002-5096-329X

Notes

The authors declare no competing financial interest.

ACKNOWLEDGMENTS

This article is dedicated to Professor Valentine Anakinov, Zelinsky Institute of Organic Chemistry, Russian Academy of Sciences, for his eminent contributions to the progress of organometallic and metal nanoparticle catalysis.

ADDITIONAL NOTE

^aLeaching values are given in mg/kg active pharmaceutical ingredients. ICP-OES limit of detection: $\text{LOD}_{\text{Pd, Si}} = 0.05$ ppm in solution or 0.50 mg/kg in the crude product.

REFERENCES

- (1) Spanova, M.; Daum, G. Squalene – biochemistry, molecular biology, process biotechnology, and applications. *Eur. J. Lipid Sci. Technol.* **2011**, *113*, 1299–1320.
- (2) Laserson, F. Neossance, 3rd Generation Squalane. *Expression Cosmetique*, 2013; pp 325–328.
- (3) Huang, Z.-R.; Lin, Y.-K.; Fang, J.-Y. Biological and Pharmacological Activities of Squalene and Related Compounds: Potential Uses in Cosmetic Dermatology. *Molecules* **2009**, *14*, 540–554.
- (4) Grand View Research. *Squalene Market Analysis by Raw Material (Vegetable, Synthetic, Animal), by Application (Food, Pharmaceuticals, Cosmetics) and Segment Forecasts to 2024*; Pune, India, 2016.
- (5) Tabur, P.; Dorin, G. US 20120040396 A1, 2012.
- (6) de Vries, E. Industrial Bioscience for Cosmetic Ingredients. How Open Innovation Advances Science. *California Chapter of the Society of Cosmetic Chemists*; San Francisco, 22 March, 2016.
- (7) Ciriminna, R.; Pandarus, V.; Béland, F.; Pagliaro, M. Catalytic Hydrogenation of Squalene to Squalane. *Org. Process Res. Dev.* **2014**, *18*, 1110–1115.
- (8) Wu, C.-S.; Tsay, Y.-J.; Liou, H.-J. Studies on the content and hydrogenation condition of squalene from the liver oil of deep sea sharks. *J. Fish. Soc. Taiwan* **1980**, *7*, 43–55.
- (9) Bonrath, W.; Medlock, J.; Schütz, J.; Wüstenberg, B.; Netscher, T. Hydrogenation in the Vitamins and Fine Chemicals Industry – An

Overview. In *Hydrogenation*; Karamé, I., Ed.; InTechOpen: Zagreb, 2012; pp 69–90.

(10) Naziri, E.; Mantzouridou, F.; Tsimidou, M. Z. Squalene resources and uses point to the potential of biotechnology. *Lipid Technol.* **2011**, *23*, 270–273.

(11) Tsujimoto, M. A Highly Unsaturated Hydrocarbon in Shark Liver Oil. *J. Ind. Eng. Chem.* **1916**, *8*, 889–896.

(12) Chapman, A. C. Spinacene: a new hydrocarbon from certain fish liver oils. *J. Chem. Soc., Trans.* **1917**, *111*, 56–69.

(13) Dale, J.; Artun, T.; Waterman, H. I.; Eliasson, N. A.; Thorell, B. Double Bond Migration and Dehydrogenation of Squalene on Hydrogenation Catalysts. *Acta Chem. Scand.* **1956**, *10*, 439–444.

(14) Fisher, K.; Schofer, S. J.; Kanne, D. B. US 20110287988 A1, 2011.

(15) Pandarus, V.; Ciriminna, R.; Kaliaguine, S.; Béland, F.; Pagliaro, M. Heterogeneously Catalyzed Hydrogenation of Squalene to Squalane under Mild Conditions. *ChemCatChem* **2015**, *7*, 2071–2076.

(16) Soni, V. K.; Sharma, R. K. Palladium-Nanoparticles-Intercalated Montmorillonite Clay: A Green Catalyst for the Solvent-Free Chemoselective Hydrogenation of Squalene. *ChemCatChem* **2016**, *8*, 1763–1768.

(17) Pagliaro, M.; Pandarus, V.; Béland, F.; Ciriminna, R.; Palmisano, G.; Carà, P. D. A new class of heterogeneous Pd catalysts for synthetic organic chemistry. *Catal. Sci. Technol.* **2011**, *1*, 736–739.

(18) Pandarus, V.; Gingras, G.; Béland, F.; Ciriminna, R.; Pagliaro, M. Selective Hydrogenation of Alkenes under Ultramild Conditions. *Org. Process Res. Dev.* **2012**, *16*, 1230–1234.

(19) Pandarus, V.; Gingras, G.; Béland, F.; Ciriminna, R.; Pagliaro, M. Selective Hydrogenation of Vegetable Oils over SiliaCat Pd(0). *Org. Process Res. Dev.* **2012**, *16*, 1307–1311.

(20) Ciriminna, R.; Sciortino, M.; Alonzo, G.; de Schrijver, A.; Pagliaro, M. From Molecules to Systems: Sol-Gel Microencapsulation in Silica-Based Materials. *Chem. Rev.* **2011**, *111*, 765–789.

(21) Sangeetha, P.; Seetharamulu, P.; Shanthi, K.; Narayanan, S.; Rama Rao, K. S. Studies on Mg-Al oxide hydrotalcite supported Pd catalysts for vapor phase hydrogenation of nitrobenzene. *J. Mol. Catal. A: Chem.* **2007**, *273*, 244–249.

(22) Leofanti, G.; Padovan, M.; Tozzola, G.; Venturelli, B. Surface area and pore texture of catalysts. *Catal. Today* **1998**, *41*, 207–219.

(23) Glaser, R. H.; Wilkes, G. L.; Bronnimann, C. E. Solid-state ^{29}Si NMR of TEOS-based multifunctional sol-gel materials. *J. Non-Cryst. Solids* **1989**, *113*, 73–87.

(24) Grunenwald, A.; Ayril, A.; Albouy, P.-A.; Licitra, C.; Gergaud, P.; Quemener, D.; Deratani, A.; Rouessac, V.; Zenasni, A.; Jousseume, V. Hydrophobic mesostructured organosilica-based thin films with tunable mesopore ordering. *Microporous Mesoporous Mater.* **2012**, *150*, 64–75.

(25) Ciriminna, R.; Pandarus, V.; Fidalgo, A.; Ilharco, L. M.; Béland, F.; Pagliaro, M. SiliaCat: A Versatile Catalyst Series for Synthetic Organic Chemistry. *Org. Process Res. Dev.* **2015**, *19*, 755–768.